Supplementary Information

Redox staining of metallic lithium inside batteries for multimodal visualization and identification with multiscale spatial resolution

Jun Ho Lee[1,†], Jane K. J. Lee[2,†], Pu Zhang[1], Sarah E. Holmes[3], Wenbo Zhang[1], Il Rok Choi[1,4], Sang Cheol Kim[1], Junyoung Lee[1], Sanzeeda Baig Shuchi[4], Mun Sek Kim[4], Zhenan Bao[4], Wah Chiu[2,5]*, Yi Cui[1,6,7]*

Corresponding author: Y.C., yicui@stanford.edu; W.C., wahc@stanford.edu

Affiliations:

[1]Department of Materials Science and Engineering, Stanford University; Stanford, CA 94305, USA

[2]Department of Structural Biology, Stanford University; Stanford, CA 94305, USA

[3]Department of Chemistry, Stanford University; Stanford, CA 94305, USA

[4]Department of Chemical Engineering, Stanford University; Stanford, CA 94305, USA

[5]Division of CryoEM and Bioimaging, SSRL, SLAC National Accelerator Laboratory; Stanford University, Menlo Park, CA 94025, USA

[6]Stanford Institute for Materials and Energy Sciences, SLAC National Accelerator Laboratory; Menlo Park, CA 94025, USA.

[7]Department of Energy Science and Engineering, Stanford University; Stanford, CA 94305, USA.

†These authors contributed equally to the paper.

*Corresponding authors, email: Y.C., yicui@stanford.edu; W.C., wahc@stanford.edu

Materials and Methods

Electrochemical analysis

Li foil (500 μm, 99.9 % (MSE Supplies)) and Cu foil (Pred Materials) were purchased and used in all electrochemical experiments. LiFSI (lithium bis(fluorosulfonyl)imide, 99 %, (Oakwood Products INC)), DME (1,2-dimethoxyethane, anhydrous 99.5% (Sigma-Aldrich)) and TTE (1,1,2,2-Tetrafluoroethyl-2,2,3,3-tetrafluoropropyl ether, 98% (Oakwood Products INC)) were purchased and used to make 1 M LiFSI in DME electrolyte and localized high concentration electrolyte (LHCE, LiFSI : DME : TTE = 1 : 1.2 : 3). 1M $LiPF_6$ (lithium hexafluorophosphate) in EC (ethylene carbonate) and DEC (diethyl carbonate) (1:1) electrolyte (LP40) was purchased from BASF. All cells were fabricated with 2032-type stainless steel coin cell cases and 40 μL of electrolyte. The Li surface was mechanically sheared with a polyethylene scrapers to remove the surface oxide layer and punched to 1 cm^2. Li||Cu and Li||Li half-cells were assembled in an Ar glove box with O_2 concentration less than 0.2 ppm, and H_2O concentration less than 0.01 ppm. Celgard 2325 PP/PE/PP trilayer was used as a separator. Cells were cycled at a current density of 1 mA cm^{-2} with a protocol of charging to 1 mAh cm^{-2} and discharging to a cutoff voltage of 1 V, unless stated otherwise, using LAND battery cycling systems at room temperature.

Staining

$AuCl_3$ (> 99.99%, trace metal basis), and $ZnCl_2$ (anhydrous, > 98%, reagent grade) salts were purchased from Sigma-Aldrich and dissolved in DME with varying concentrations of 0.01, 0.05, and 0.1 M inside an Ar-filled glovebox. Cells were disassembled in the glovebox and 20 μL of the staining solution was dropped onto the anode for at least 30 seconds. In the case of residual SEI, the staining time was set to be longer (> 2 min) for better wetting. After staining, the electrodes were washed with 100 μL of DME solvent to remove the remaining staining precursor and salts of the electrolyte. The samples were dried in an Ar-filled glovebox at room temperature for further analysis.

SEM-EDS analysis

SEM-EDS analysis was conducted on the Thermo Fisher Scientific Apreo S LoVac Scanning Electron Microscopy equipped with the Bruker Quantax XFlash 6 | 60 SDD EDS detector. For SEM analysis, cells were disassembled in an Ar glovebox and rinsed with 100 μL of DME solvent to remove remaining salt from the electrolyte. Cross-sectional samples were prepared by ripping them with a blade. After drying, samples were mounted on the SEM holder and transferred to SEM with a minimal air exposure (< 1 min). Everhart-Thonley Detector was used for SEM images at 10 kV, unless mentioned otherwise. Obtained EDS maps of samples were further imported into ImageJ to transform into binary images to locate regions with high signals.

Thin film deposition

Al_2O_3 was deposited on Cu current collector using Arradiance Gemstar 6 ALD reactor. Trimethylaluminum (TMA) was used as the metal-organic precursor and water (H_2O) was the counter reactant. 30 mS pulses of each precursor were used for an ALD cycle in the sequence: TMA pulse-purge-water pulse-purge. The temperature was 150 °C, which resulted in a growth rate of ~1.1 Å per cycle.

X-ray diffraction of nanoparticles before/after staining

X-ray diffraction with Li_2O (Nanoshel), LiF (Nanoshel), Li_2CO_3 (Nanoshel) and PEO (Sigma-Aldrich) nanoparticles were conducted with Empyrean X-ray Diffractometer (PANalytical B.V.) using Cu source at 45 kV and 40 mA. XRD spectra were collected from 10^o to 70^o at a step of 0.00715^o. Stained samples were prepared by dropping 50 mM AuCl3 DME solution to powder followed by washing with DME. Powder samples were fully dried before loading on to cavity glass slides for XRD.

Cryo-EM and cryo-ET

For cryo-EM analysis, we used Quantifoil copper R2/2 grids, carbon film 200 mesh (SPI) without any surface treatment. Cells plated Li for 0.1 mAh cm^{-2} at 1 mA cm^{-2} were disassembled inside the glove box and stained afterwards. The electrode with stained dendrites was sonicated in DME solvent for 15 min and 20 µL of the dispersed solution was pipetted onto the grid, followed by manual blotting of the grids with filter paper (Whatman). After blotting the grid, we transferred the grid into a small 0.2 mL tube (Thermo Fisher) and used parafilm to wrap the tube to prevent oxygen contamination. Then we rapidly transported the tube from the glovebox into liquid nitrogen, immersing the TEM grid in liquid nitrogen. Afterwards, the grid was transferred to a cryoEM grid box and moved to a loading station to be subsequently loaded into the microscope.

EELS and EDX spectroscopy and STEM imaging were performed on the Thermo Fisher Spectra Double-Corrected Transmission Electron Microscope, operated at 300kV. EELS and EDX spectroscopy were performed simultaneously using the Velox software and the Gatan Digital Micrograph software. The EDX image was filtered with a 5-pixel filter. HR-TEM images of the stained dendrite were collected on the FEI Titan Environmental Transmission Electron Microscope operated at 300 kV. The cryo-ET tilt series was collected from the Krios G2 300kV Cryo-Transmission Electron Microscope, with a Selectris imaging filter and a Falcon 4i Direct Electron Detector. For the tilt series, the dose rate per image was 1.0 $e/Å^2 \cdot sec$ at a magnification of 15000X, with one image being taken at every 1° tilt from +60° to -60°. The tomogram was reconstructed with IMOD (1-2) and segmented into Dragonfly Pro software (2).

X-ray computed tomography

Micro-CT imaging was performed using a Zeiss Xradia 520 Versa X-ray instrument (Carl Zeiss Inc., CA, USA). The system, equipped with a polychromatic micro-focus sealed source, operated at 50 kV and 4 W on a tungsten target. A 20× objective lens coupled with a scintillator projected images onto a 2048 × 2048-pixel CCD detector. With 2× pixel binning, this setup achieved a pixel size of ≈0.71 µm and a field of view of ≈708 µm.

Sample preparation involved extracting lithium samples of interest with a 1 mm diameter biopsy punch and sealing them in 100 µm wall thickness, 1.003 mm inner diameter polyimide tubes to prevent air exposure. The proximity of the sample to the detector ensures minimum beam attenuation. During imaging, the sealed sample rotated 360°, capturing 3000 radiographs at regular angular intervals with exposure times of 4 s.

Image reconstruction utilized the Zeiss XMReconstructor software (Carl Zeiss Inc.), employing a modified Feldkamp–David–Kress (FDK) algorithm for cone beam geometry (3). Subsequent 3D analysis, including filtering and segmentation, was conducted using Dragonfly Pro software (4).

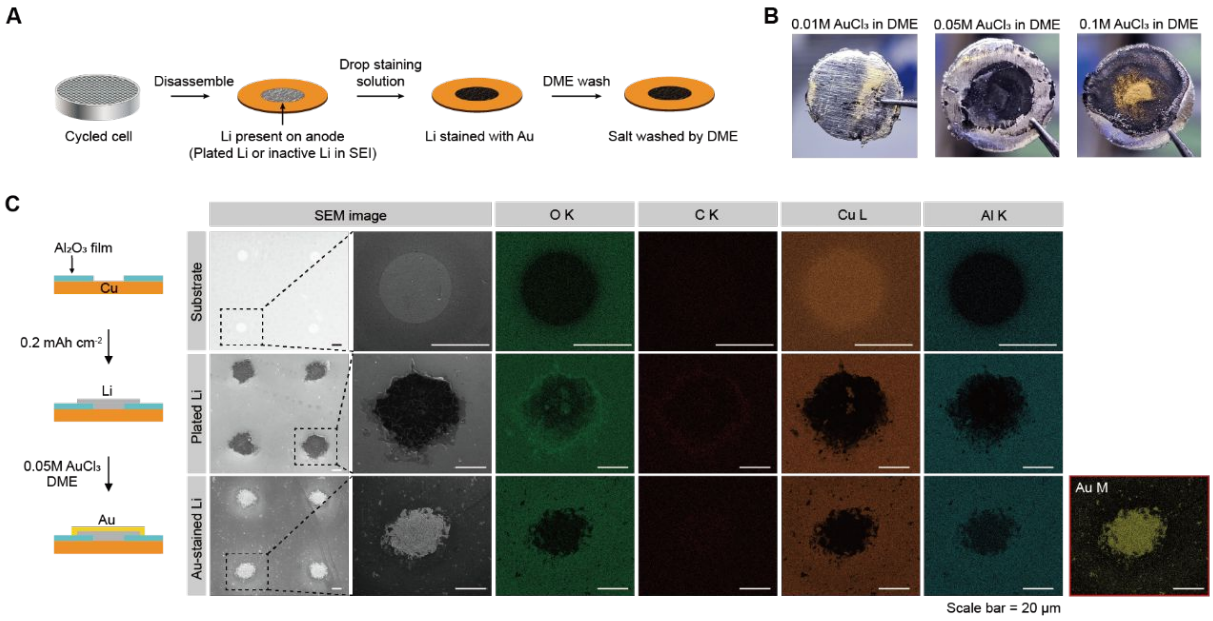

Fig. S1. Validation of the staining on Li^0.

A, Schematic representation of staining procedure. **B**, Optical images showing color changes on the surface of Li^0 (1 cm^2) 3 minutes after dropping 20 μL of different concentrations of the staining solution. Regions in black represent the area covered by the solution. 0.01 M of the solution only exhibited small color change (left), whereas 0.1 M of the solution significantly changed the surface color (black) with precipitation (yellow) at the center (right). 0.05 M was chosen as the optimal concentration due to the uniformity of the surface color and the reaction time. **C**, Representative images of the modeled substrate at each stage (left column) and their corresponding SEM-EDS images (right matrix). Dotted black boxes on the first SEM images of each row mark the enlarged regions for the second left SEM images. Scale bar = 20 μm.

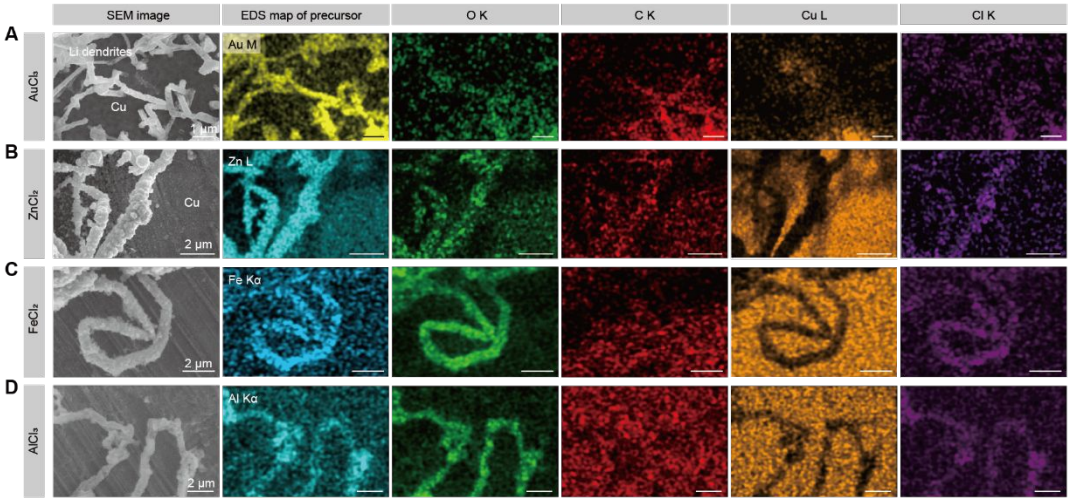

Fig. S2. SEM and EDS analysis on stained Li^0 dendrites.

Li^0 was plated to 0.25 mAh cm^{-2} at 1 mA cm^{-2} on Cu current collector in 1M LiFSI DME electrolyte. Plated Li^0 on Cu were retrieved from disassembled cells and stained with DME solution of each precursor for 3 min. SEM image and corresponding EDS maps of Li stained with 50 mM of $AuCl_3$ solution (**A**), 50 mM of $ZnCl_2$ solution (**B**), $FeCl_2$ solution (**C**), and $AlCl_3$ solution (**D**). Despite extremely low solubilities of $FeCl_2$ and $AlCl_3$ in DME, both Fe and Al EDS maps displayed strong signals correlated to dendrites in respective SEM images measured at 15 kV.

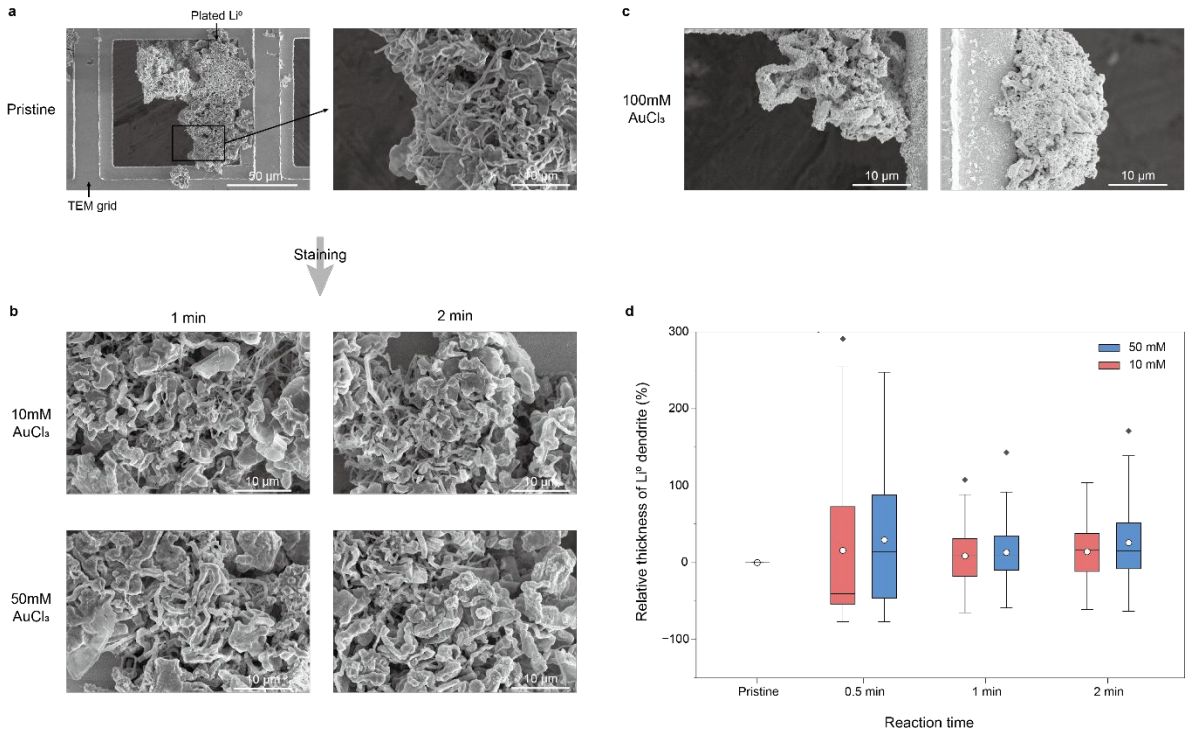

Fig. S3. Statistical analysis on morphological changes of Li^0 with redox staining. a, SEM images of Li^0 plated on Cu grid (left, 0.2 mAh cm^{-2} plated at 2 mA cm^{-2}, 1M LiFSI in DME) and zoomed in image of the boxed region (right). b, SEM images of Li^0 dendrites after redox staining with $AuCl_3$ in DME solution. Images of dendrites from different staining concentrations (10 mM and 50 mM) and reaction times (1 min and 2 min). scale bar = 10 µm. c, SEM images of Li^0 dendrites after redox staining with 100 mM $AuCl_3$ in DME solution. Images from two different locations are shown. scale bar = 10 µm. d, Plot showing average thickness of Li^0 dendrites. Boxes in red and blue represent thickness distribution of dendrites stained with 10 mM and 50 mM $AuCl_3$ solution, respectively. A white circle in each box shows average value in each set. Minimum of 100 dendrites in total are randomly selected from at least 3 different spots in each case. Results with 100 mM $AuCl_3$ solution are not considered.

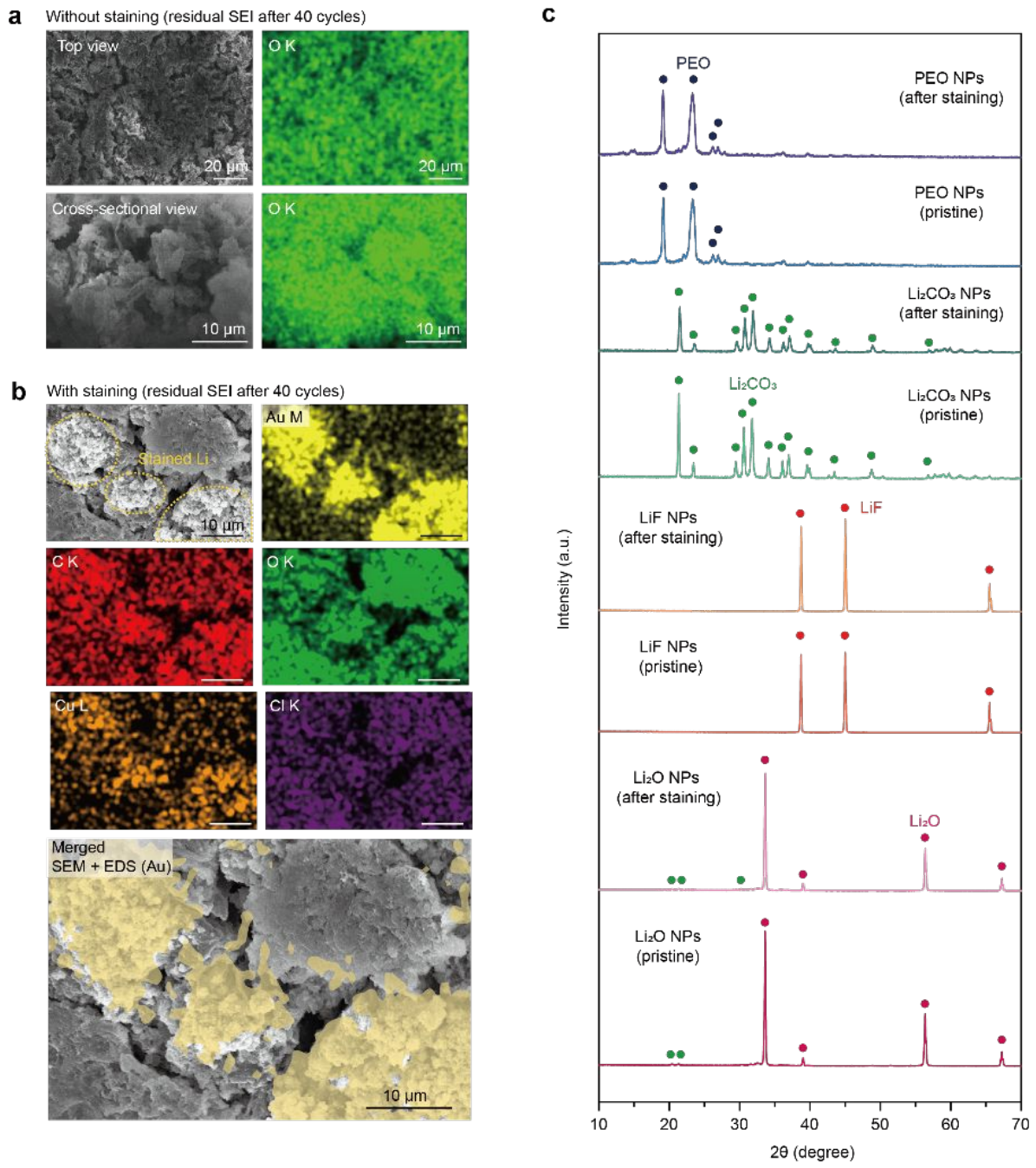

Fig. S4. Selectivity of staining on Li^0 over residual SEI.

a, Representative SEM and corresponding EDS O K maps of residual SEI after 40 cycles without staining. Both top-view (left) and cross-sectional (right) images exhibited complex microstructures of inactive Li^0 and residual SEI. EDS O K maps were not sufficient to distinguish Li^0 from SEI. **b**, Representative SEM and corresponding EDS maps of residual SEI after 40 cycles followed by staining with Au. The merged image of SEM, and EDS Au M map

(yellow) was shown on the right. Li||Cu half-cells were cycled at 1 mA cm^{-2} with a plating capacity of 0.5 mAh cm^{-2}. **d**, XRD spectra of Li_2O (pink), LiF (orange), Li_2CO_3 (green), and PEO (blue) nanoparticles (NPs) before and after staining with $AuCl_3$ solution. Standard peaks of Li_2O (pink), LiF (orange), and Li_2CO_3 (green), and PEO (navy) were depicted. No peaks related to Au were visible after 2 mins of reaction.

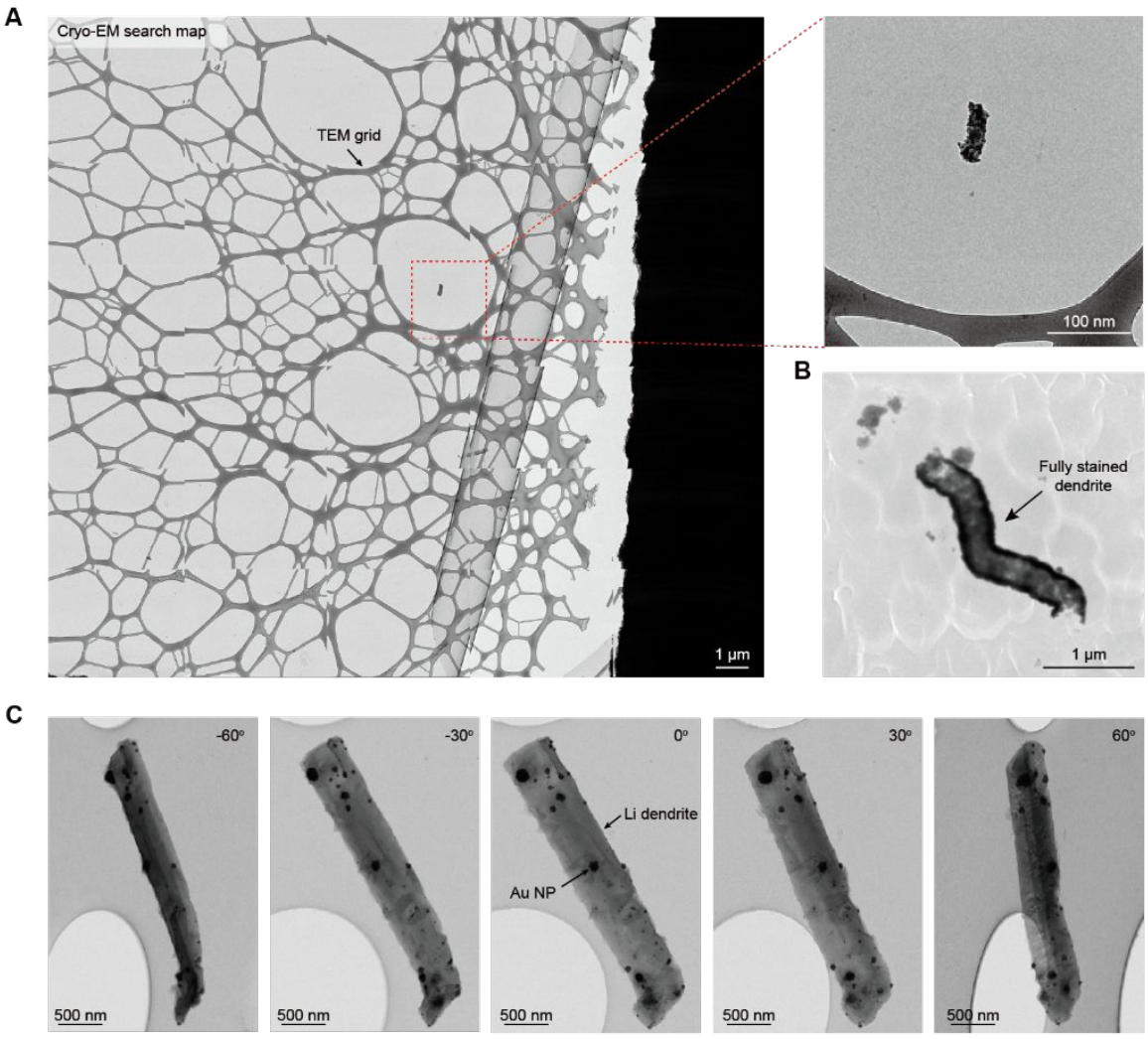

Fig. S5. Cryo-EM images of stained dendrites.

A, Search map of a stained dendrite on lacey carbon TEM grids under cryo-EM. A red dotted box marks the region with the stained dendrite and the enlarged image is shown on the right. **B**, cryo-EM image of fully stained dendrite. The time of staining was increased to 1 hr to completely cover the surface of a dendrite. **C**, Tilt series of stained dendrite obtained by tilting the TEM stage from -60 to 60 degrees. Black dots on the dendrite represent Au NPs. Cells were cycled 5 times at 1 mA cm^{-2} for 1 mAh cm^{-2}.

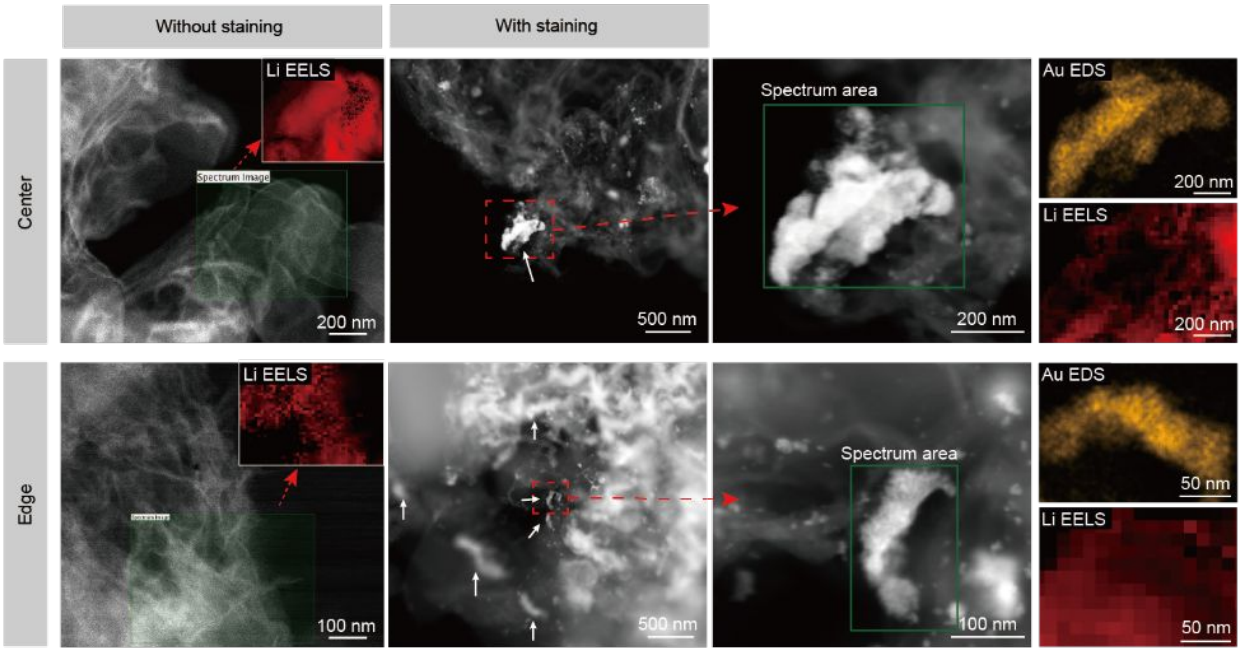

Fig. S6. Cryo-EM images of residual SEI with and without staining.

Cryo-EM images of residual SEI collected from the center (top row) and the edge (bottom row) of anodes cycled with 1M DME electrolyte. The left and the right column show samples without and with staining using $AuCl_3$ solution. White arrows mark the location of stained Li dendrites. EELS (Li K) and EDS map (Au) on the right were from the red boxed regions. Cells were cycled 5 times at 1 mA cm^{-2} for 1 mAh cm^{-2}.

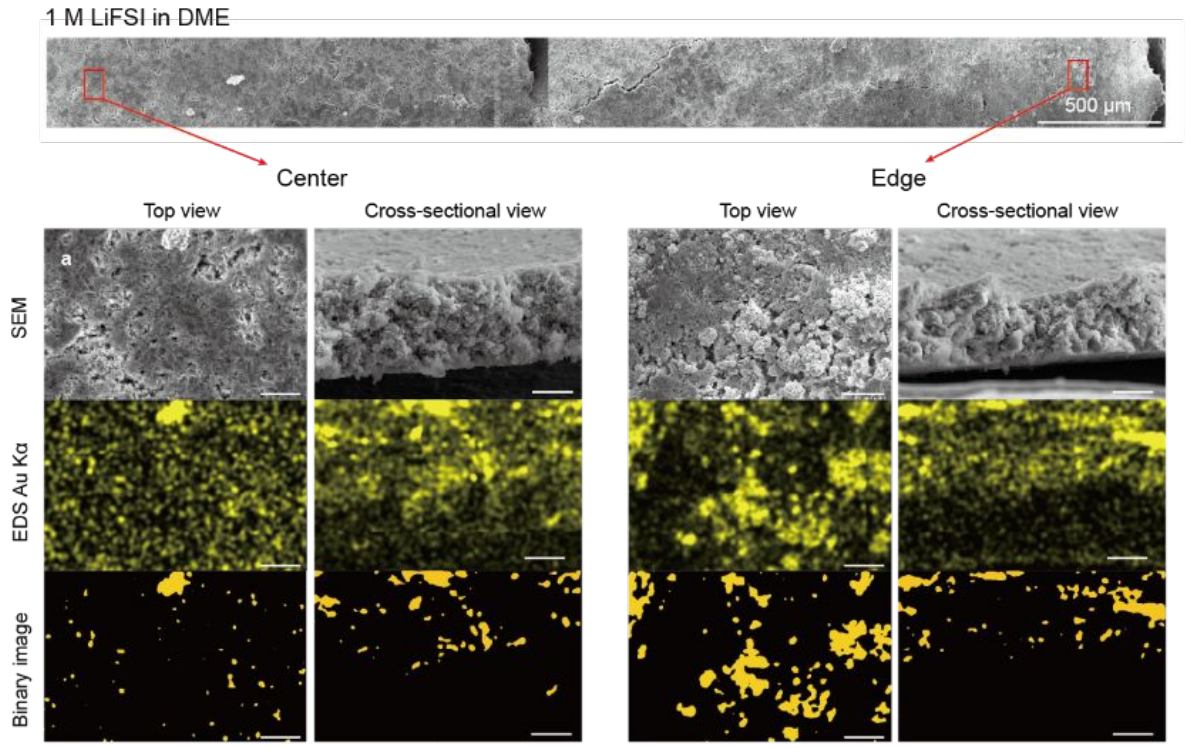

Fig. S7. SEM-EDS analysis on various locations of residual SEI in 1M LiFSI in DME electrolyte with staining

(Top) Line scan of residual SEI cycled with 1 M LiFSI in DME electrolyte. Each integrated image was obtained by performing SEM on consecutive locations and combining them. Boxes in red represent enlarged SEM images at the center (left) and the edge (right), respectively. (Bottom) SEM images, EDS O K maps, and binary images from EDS maps of residual SEI at the center (left) and the edge (right). Both top view and cross-sectional view images are shown from the same location. Scale bar = 20 μm.

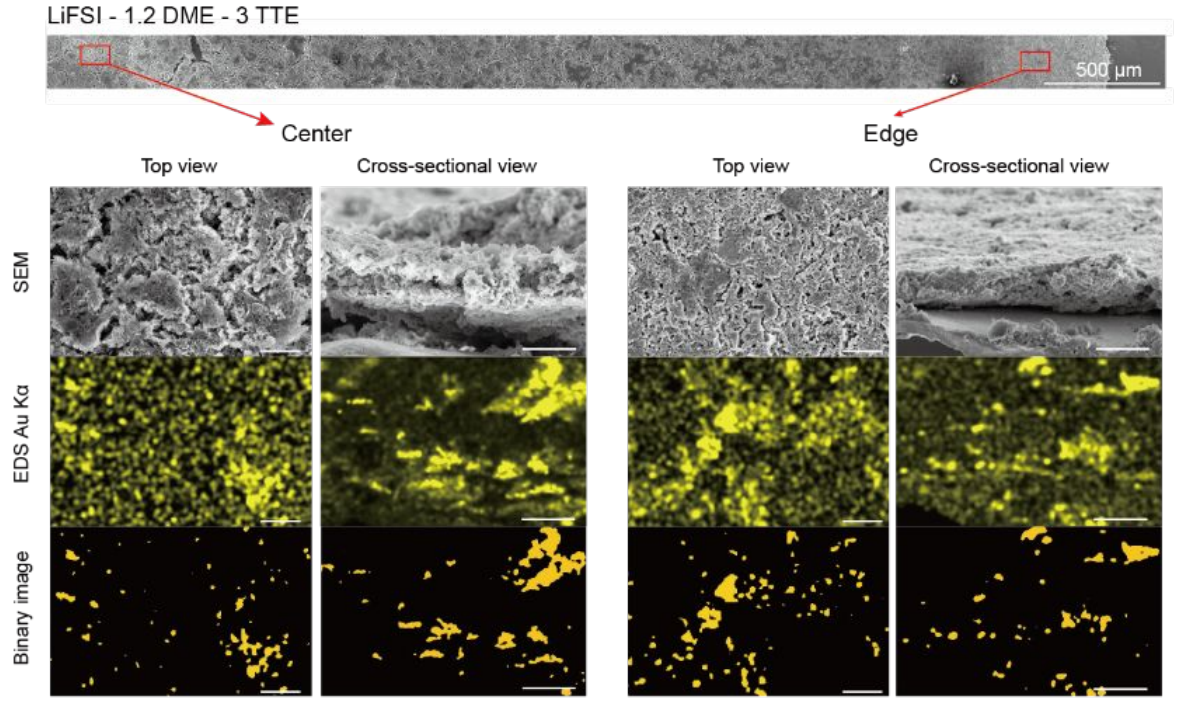

Fig. S8. SEM-EDS analysis on various locations of residual SEI in LiFSI – 1.2 DME – 3 TTE electrolyte with staining

(Top) Line scan of residual SEI cycled with LiFSI – 1.2 DME – 3 TTE electrolyte. Each integrated image was obtained by performing SEM on consecutive locations and combining them. Boxes in red represent enlarged SEM images at the center (left) and the edge (right), respectively. (Bottom) SEM images, EDS O K maps, and binary images from EDS maps of residual SEI at the center (left) and the edge (right). Both top view and cross-sectional view images are shown from the same location. Scale bar = 20 µm.

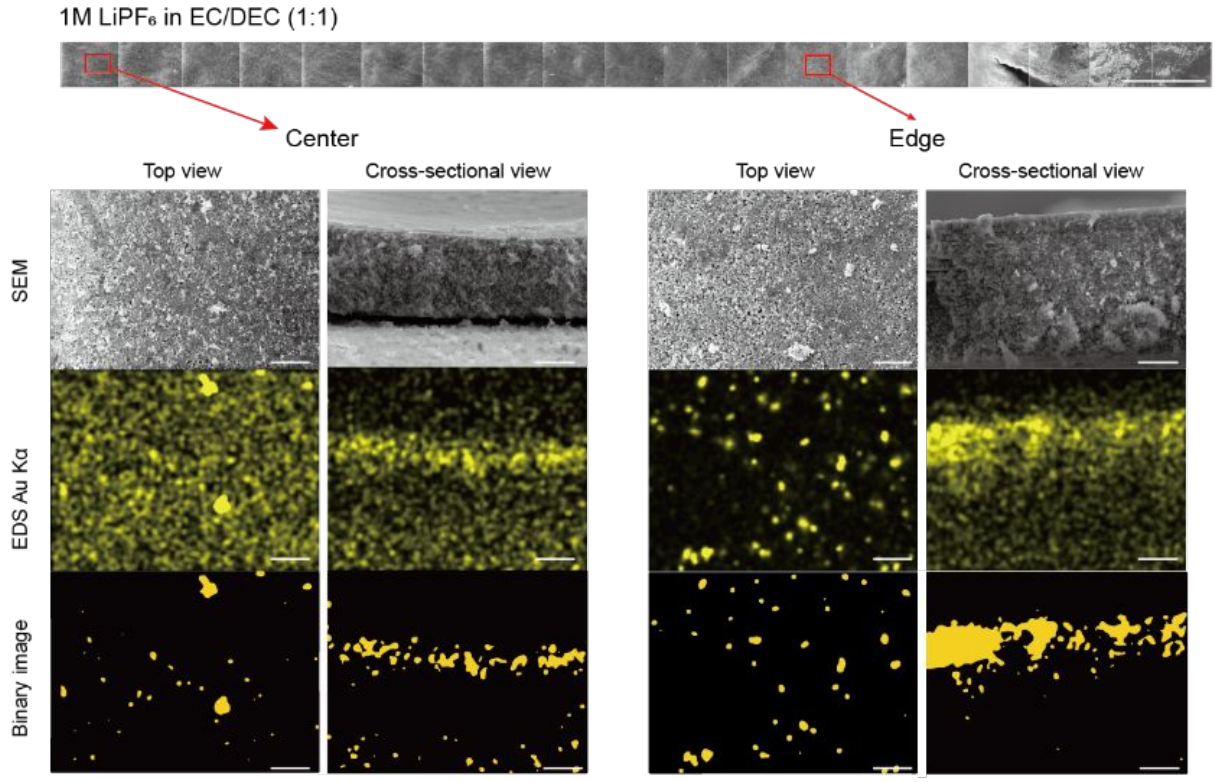

Fig. S9. SEM-EDS analysis on various locations of residual SEI in 1M $LiPF_6$ in EC/DEC (1:1) electrolyte with staining

(Top) Line scan of residual SEI cycled with 1 M $LiPF_6$ in EC/DEC (1:1) electrolyte. Each integrated image was obtained by performing SEM on consecutive locations and combining them. Boxes in red represent enlarged SEM images at the center (left) and the edge (right), respectively. (Bottom) SEM images, EDS O K maps, and binary images from EDS maps of residual SEI at the center (left) and the edge (right). Both top view and cross-sectional view images are shown from the same location. Scale bar = 20 μm.

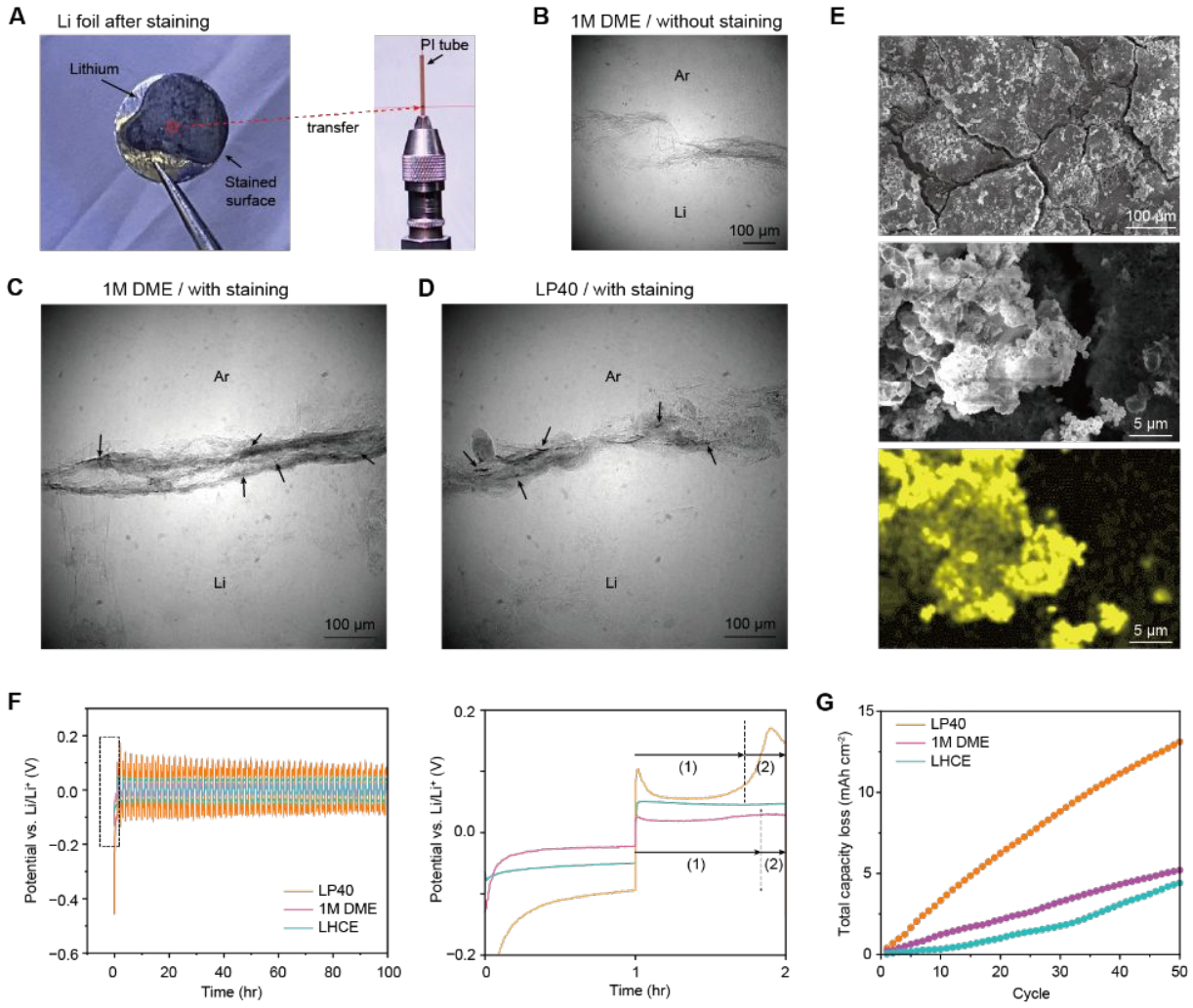

Fig. S10. XCT analysis if unstained and stained residual SEI.

A, Optical image of Li foil after staining with Au (left). The stained region is shown in black. The red circle marks the punched area of the foil for further XCT experiments. Optical image of the sample transferred to the polyimide (PI) tube and the stage is shown on the right figure. The inner diameter of the tube is 1 mm. **B**, XCT image of residual SEI on Li foil without staining the surface. The cell was cycled 50 times in 1M DME electrolyte. Li^0 (bottom) showed similar contrasts to Ar gas in headspace, and the darker contrast (middle) corresponded to residual SEI. Residual SEI exhibited a darker contrast than Li due to heavier elements present in it. **C-D**, XCT images of residual SEI on Li foil in 1 M DME (**C**), and LP40 (**D**) electrolyte with staining. Black dots or areas indicated by arrows corresponded to stained inactive Li^0. They displayed significantly darker contrast than Li^0 or residual SEI. **E**, SEM images of residual SEI in LP40 electrolyte after staining in large scale (top) and smaller scale (middle). The EDS Au M map of the middle is shown at the bottom. **F**, Representative cycling profiles of LP40 (orange), 1M DME (pink), and LHCE (cyan) for 50 cycles (left). The black dotted box marks the voltage profiles of the 1st cycle (right). (1) and (2) represent the stripping steps where the capacity is from the plated Li^0 and Li^0 reservoir, respectively. Overpotentials increase rapidly in (2) due to

the resistance from residual SEI, and the capacity from (2) could be considered as capacity loss[43]. **G**, Total capacity loss in LP40 (orange), 1M DME (pink), and LHCE (cyan) over 50 cycles. Total capacity loss is calculated by adding the capacity of each step (2) in **F**.

Movie S1.

3D reconstructed tomogram of a stained Li dendrite. Au NPs (yellow) are located on the surface of a Li dendrite (dark cyan).

Movie S2.

3D reconstruction of Au-stained Li surface. Au-stained surface on top of Li foil is highlighted in yellow. Li is not visible due to its high transparency to X-ray. Diameter of the top surface is 650 μm.

Movie S3.

3D reconstruction of unstained residual SEI after cycling in 1M DME electrolyte. Residual SEI is highlighted in grey while Li is not visible due to its high transparency to X-ray. Diameter of the top surface is 650 μm.

Movie S4.

3D reconstruction of Au-stained residual SEI after cycling in 1M DME electrolyte. Au-stained Li particles and residual SEI are highlighted in yellow and grey, respectively, while Li is not visible due to its high transparency to X-ray. Diameter of the top surface is 650 μm.

Movie S5.

3D reconstruction of Au-stained residual SEI after cycling in LP40 electrolyte. Au-stained Li particles and residual SEI are highlighted in yellow and grey, respectively, while Li is not visible due to its high transparency to X-ray. Diameter of the top surface is 650 μm.

Movie S6.

3D reconstruction of Au-stained residual SEI after cycling in LHCE electrolyte. Au-stained Li particles and residual SEI are highlighted in yellow and grey, respectively, while Li is not visible due to its high transparency to X-ray. Diameter of the top surface is 400 μm.

References

1. Kremer J.R., Mastronarde, D.N., and McIntosh, J.R. Computer visualization of three-dimensional image data using IMOD. *J. Struct. Biol.* **116,** 71-76 (1996).

2. Mastronarde, D.N., Dual-axis tomography: an approach with alignment methods that preserve resolution. *J. Struct. Biol*. **120**, 343-352 (1997).

3. Mastronarde, D.N. and Held, S.R., Automated tilt series alignment and tomographic reconstruction in IMOD. *J. Struct. Biol*. **197** 102-113 (2017).

4. Dragonfly 3D World, https://www.theobjects.com/dragonfly/dfhelp/2024-1/Default.htm (accessed 2024-06-01), Object Research Systems (ORS) Inc.